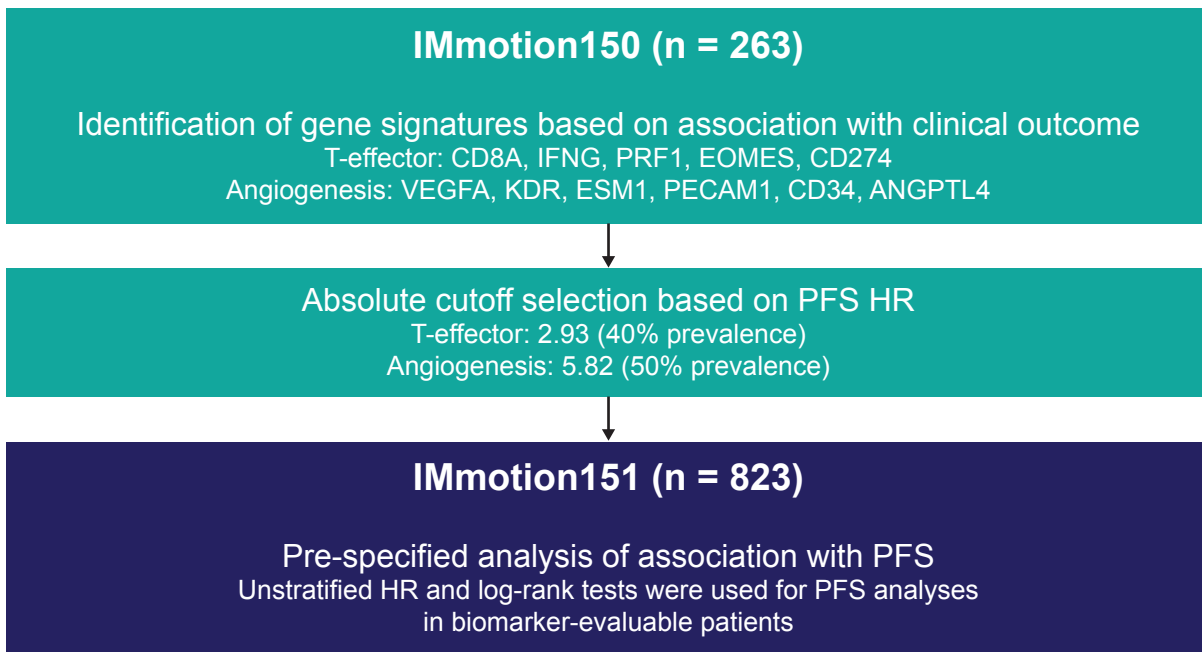
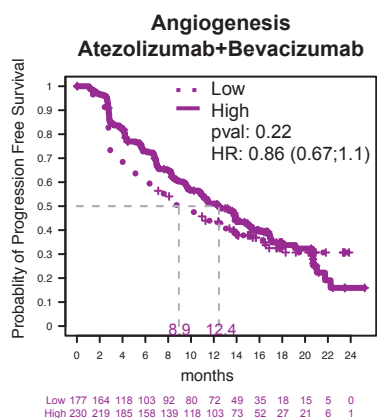


Figure S1

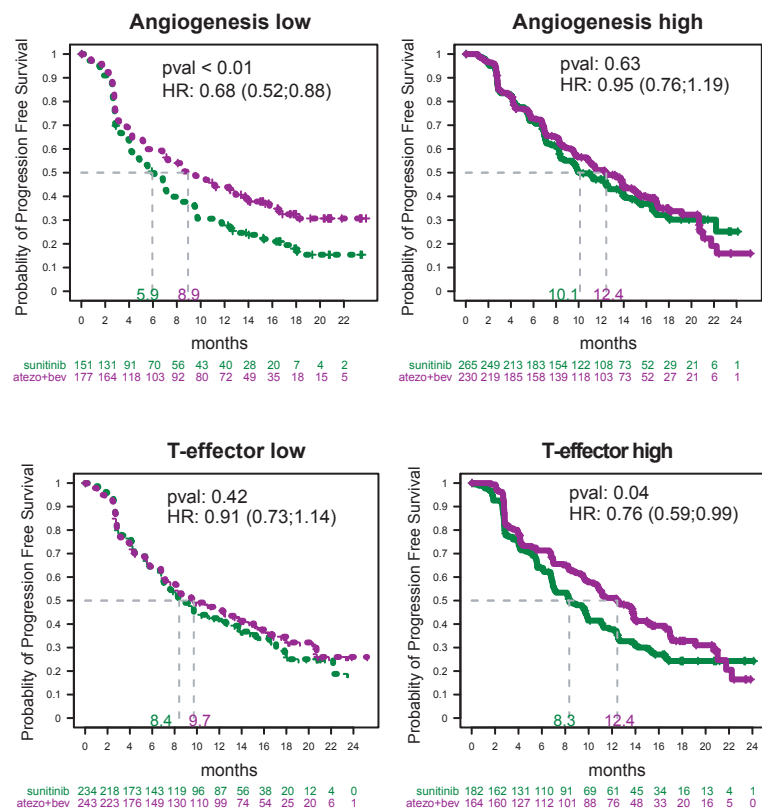
A



B



C

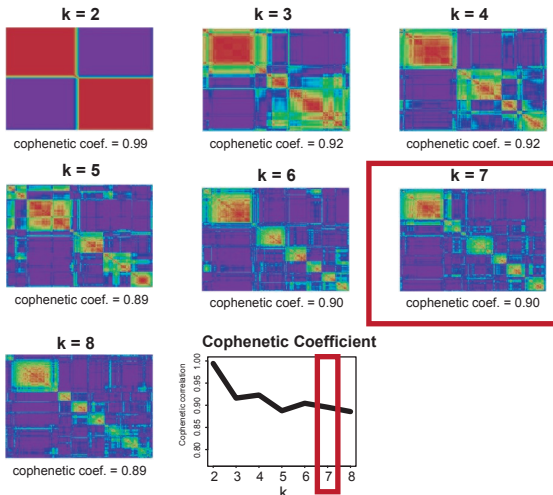


— Atezolizumab+Bevacizumab
— Sunitinib

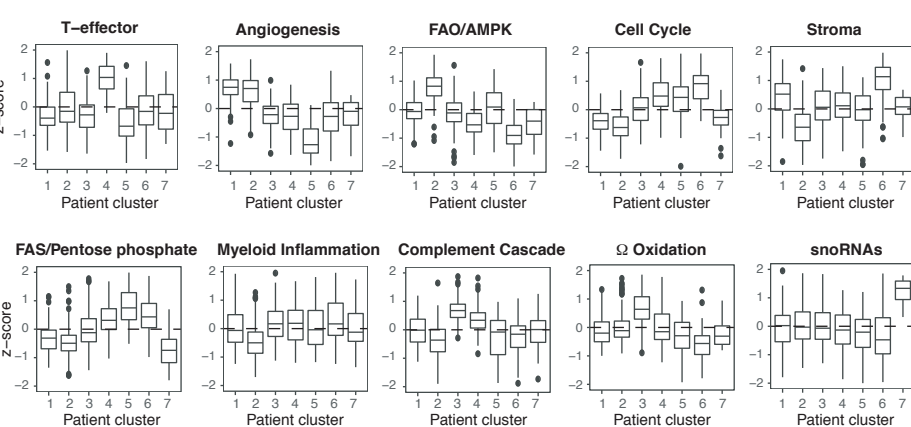
Figure S1: Validation of angiogenesis and T-effector transcriptional signature from IMmotion150 in IMmotion151, Related to STAR Methods. **A.** Workflow depicting the validation strategy for Angiogenesis and T-effector signatures established in IMmotion150. **B.** Kaplan-Meier curves of progression free survival (PFS) by treatment arm (*purple*, atezolizumab+bevacizumab; *green*, sunitinib) in patients with angiogenesis low (interrupted line) or high (continuous line) tumors. **C.** Kaplan-Meier curves of PFS by treatment arm (*purple*, atezolizumab+bevacizumab; *green*, sunitinib) in patients with angiogenesis low or high and patients with T-effector low or high tumors.

Figure S2

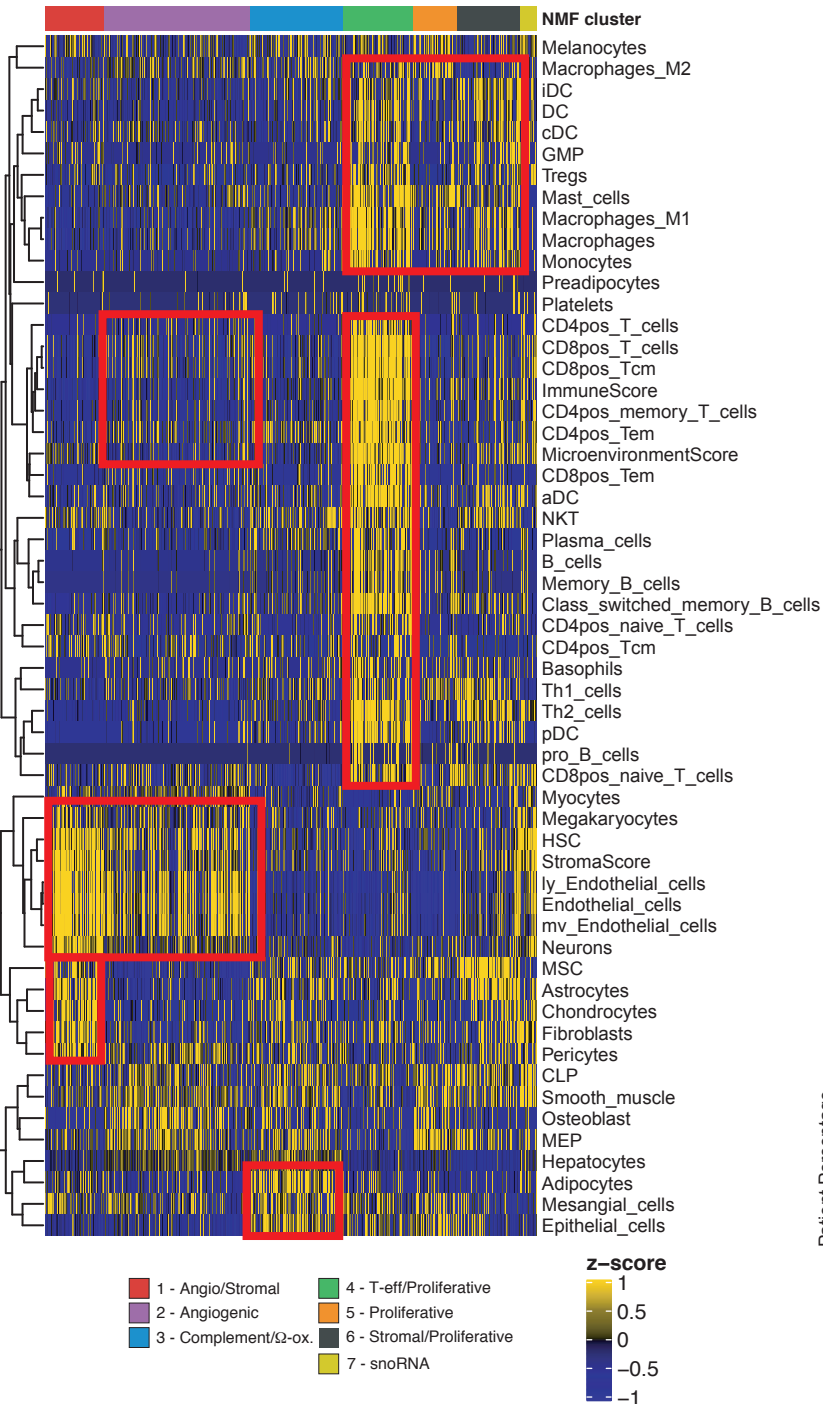
A



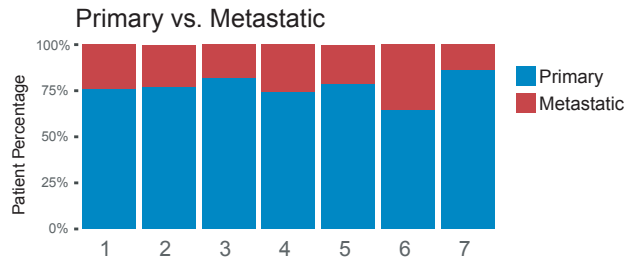
B



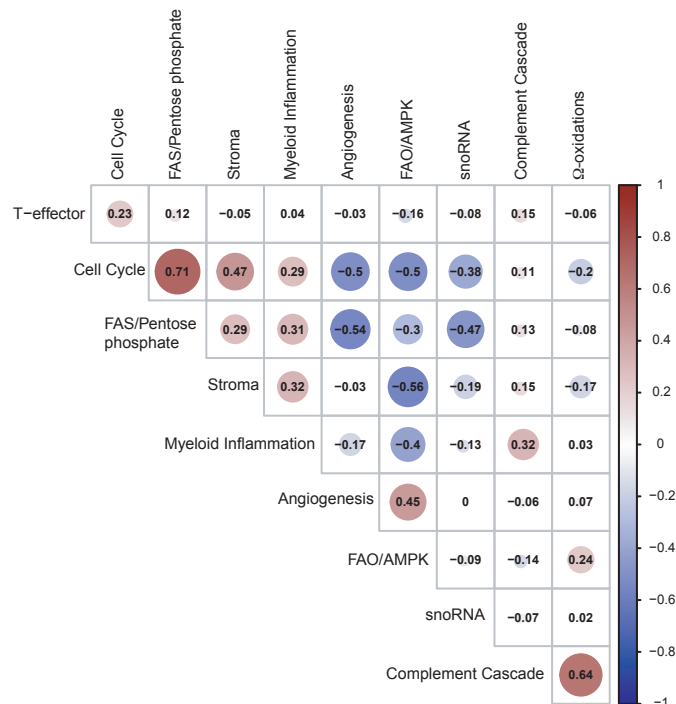
C



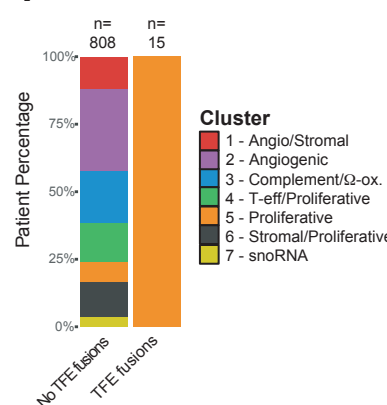
D



E



F



G

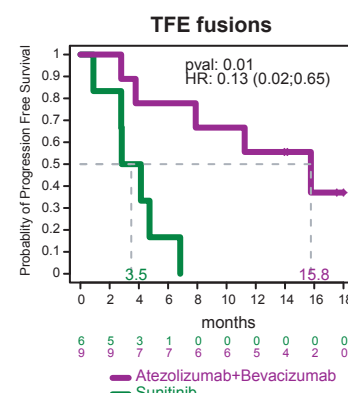
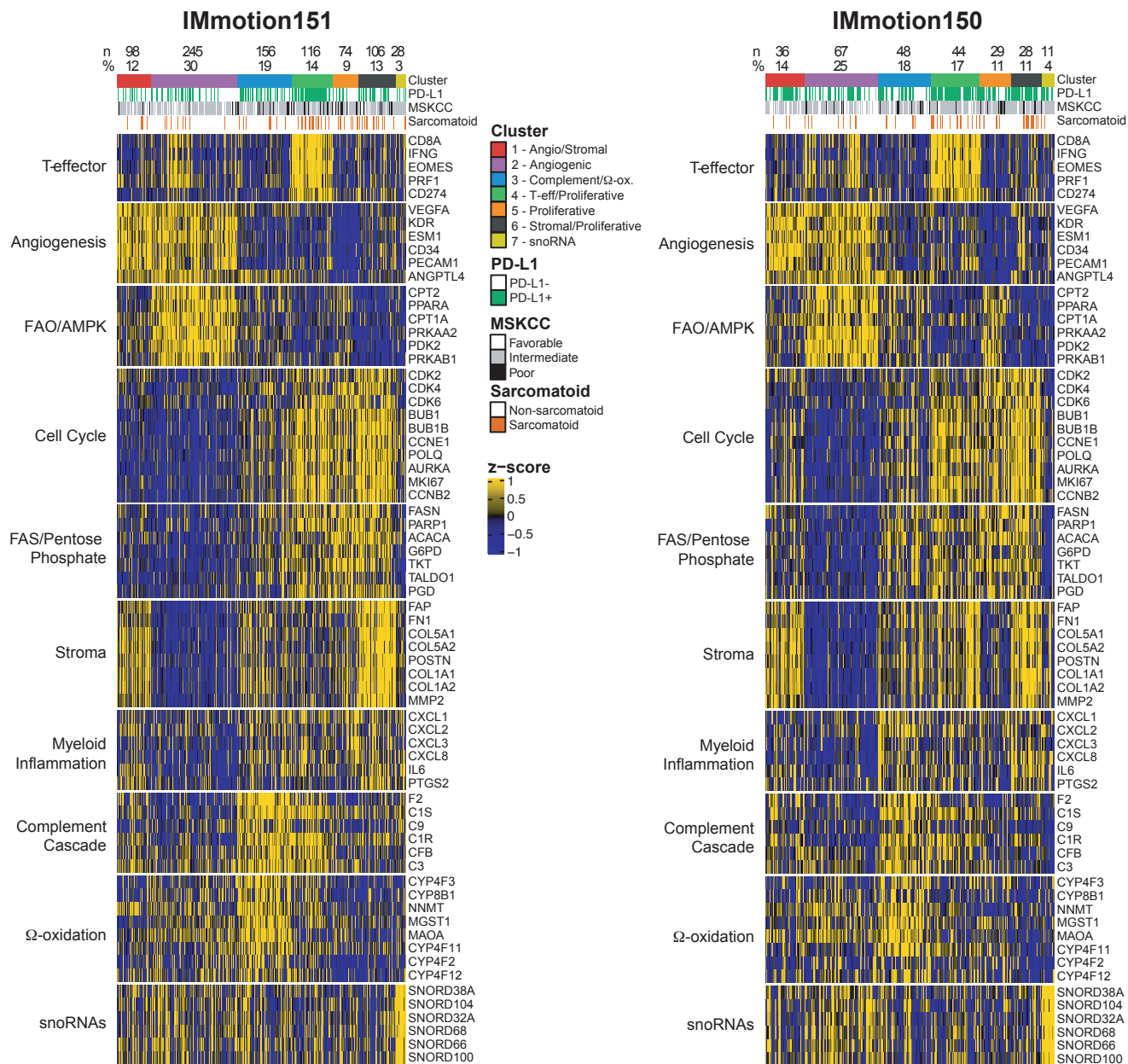


Figure S2: Non-negative matrix factorization (NMF) cluster analysis, Related to Figure 1.

A. Selection of cluster number based on consensus matrices for k=2 to k=8, and measure of cophenetic coefficient stability at various values of k. k=7, with a cophenetic coefficient of 0.90, was chosen. **B.** Transcriptional z-scores for the 10 signatures presented in the heatmap in Figure 1D were represented as boxplots by patient cluster. **C.** Hierarchical clustering of deconvolution z-scores obtained from xCell. Samples are ordered by NMF cluster. **D.** Distribution of primary and metastatic tumors in NMF clusters. **E.** Correlations between transcriptional signatures across IMmotion151 data set. Signature z-scores were computed for each of the 823 samples from IMmotion151 and Pearson correlations between signatures were calculated in a pairwise fashion. Positive and negative correlations are shown as *red* and *blue* circles respectively. The diameter of the circles is proportional to the absolute Pearson R value, which is also numerically displayed in the circles. **F.** Barchart representing the distribution of NMF clusters in tumors with or without *TFE* fusions. Fusions in *TFE3* and *TFEB* were grouped together. Tumors from 12 patients had *TFE3* fusions and 3 patients had *TFEB* fusions. **G.** Kaplan-Meier curve of progression free survival (PFS) by treatment arm (*purple*, atezolizumab+bevacizumab; *green*, sunitinib) in patients with *TFE*-fusions

Figure S3

A



B

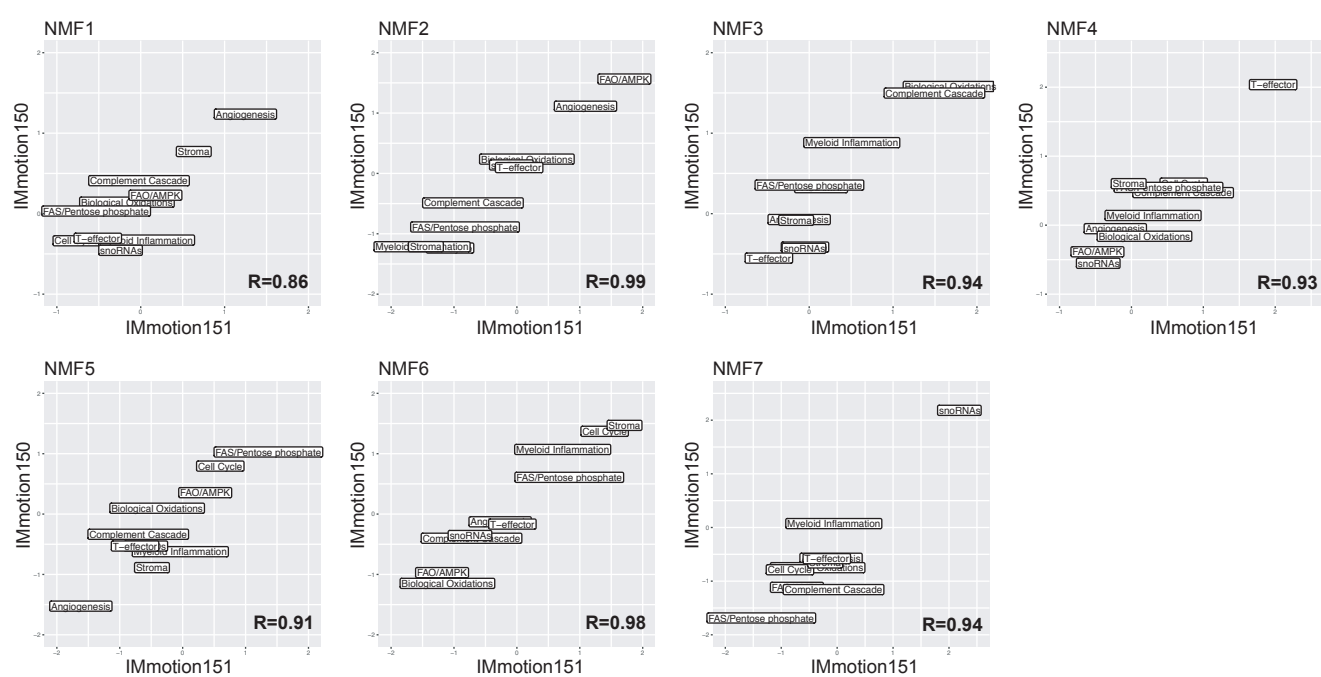
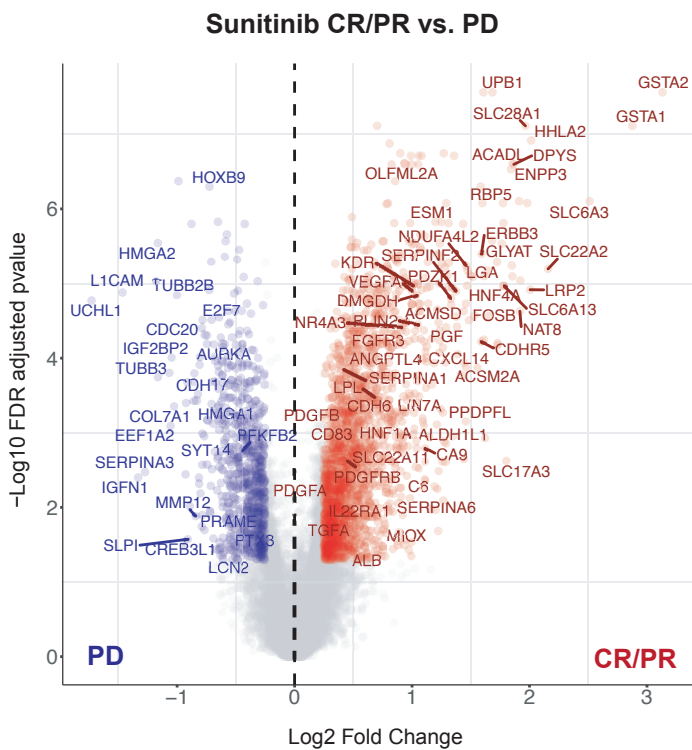


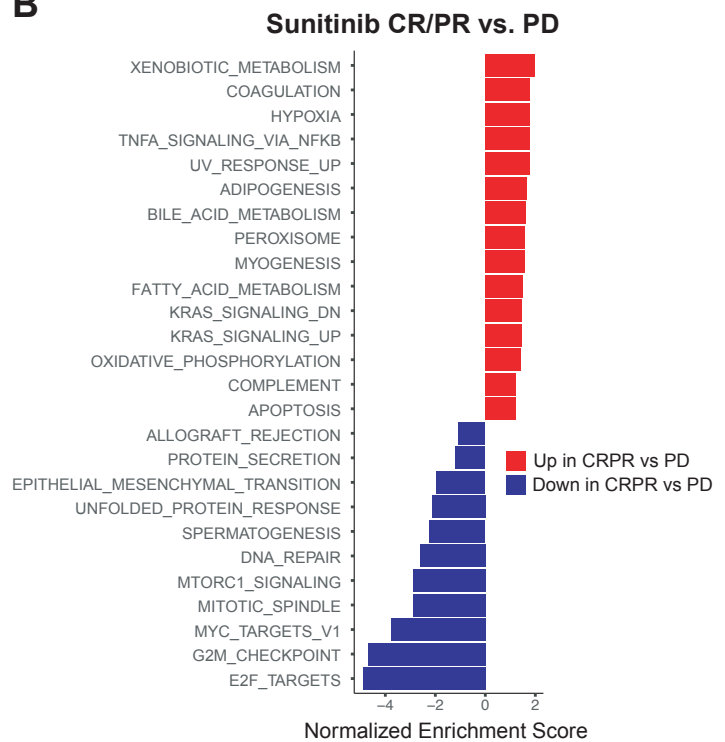
Figure S3: Validation of non-negative matrix factorization (NMF) clusters in IMmotion150, Related to Figure 1. A machine learning algorithm using random forest was developed to train a model in IMmotion151 to classify patients into NMF groups based on the 3,072 (top 10%) most variable genes in this data set (STAR Methods). This model was applied to assign patients from IMmotion150 into each cluster. **A.** The heatmap generated in Figure 1D in IMmotion151 (*left panel*) was then derived in IMmotion150 (*right panel*). Signature patterns across patient clusters were highly conserved between IMmotion151 and IMmotion150 datasets. **B.** X-Y charts representing the mean aggregate z-score for our ten transcriptional signatures in IMmotion151 (x-axis) and IMmotion150 (y-axis) for each NMF group. The Pearson R value is represented on each plot.

Figure S4

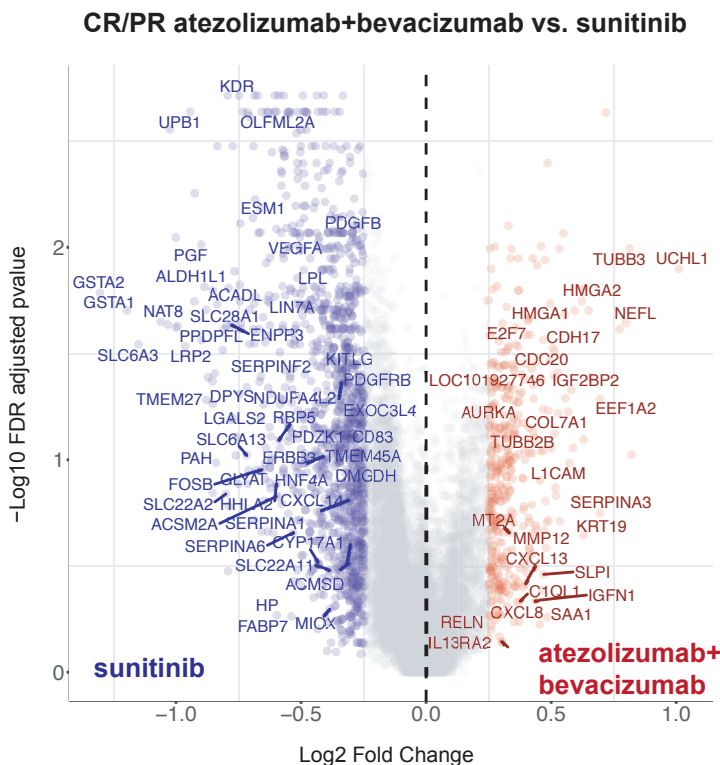
A



B



C



D

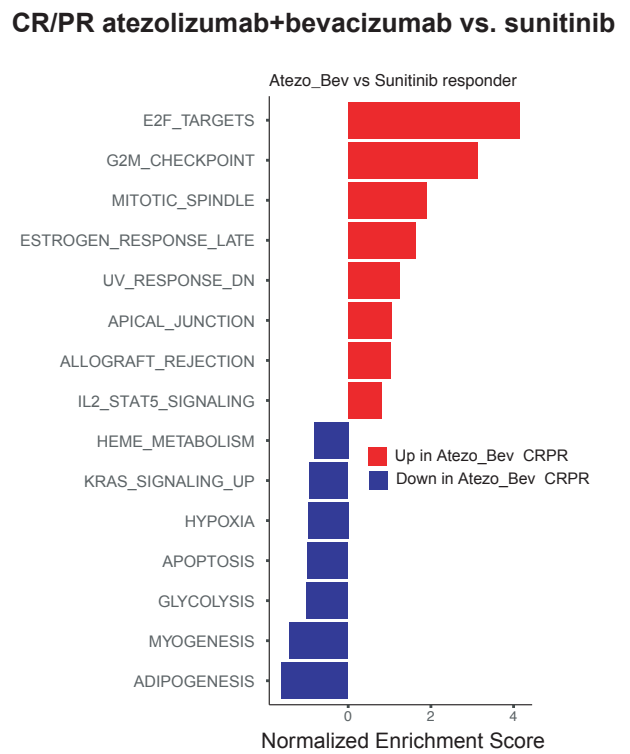


Figure S4: Analysis of differentially expressed genes and pathways in responder vs. non-responder patients, Related to Figure 2. **A.** Volcano plot depicting differentially expressed genes between responders (CR/PR) and non-responders (PD) in the sunitinib arm. Genes with FDR-corrected $p < 0.05$ and absolute log-fold change ≥ 0.25 are represented in red or blue. **B.** Bar chart representing pathway enrichment scores for the top upregulated or downregulated MSigDb hallmark gene sets within the differentially expressed genes identified in A. **C.** Volcano plot depicting differentially expressed genes in responders (CR/PR) treated with atezolizumab+bevacizumab or sunitinib. Genes with FDR-corrected $p < 0.05$ and absolute log-fold change ≥ 0.25 are represented in red or blue. **D.** Bar chart representing pathway enrichment scores for the top upregulated or downregulated MSigDb hallmark gene sets within the differentially expressed genes identified in C. CR, complete response; PR, partial response; PD, progressive disease.

Figure S5

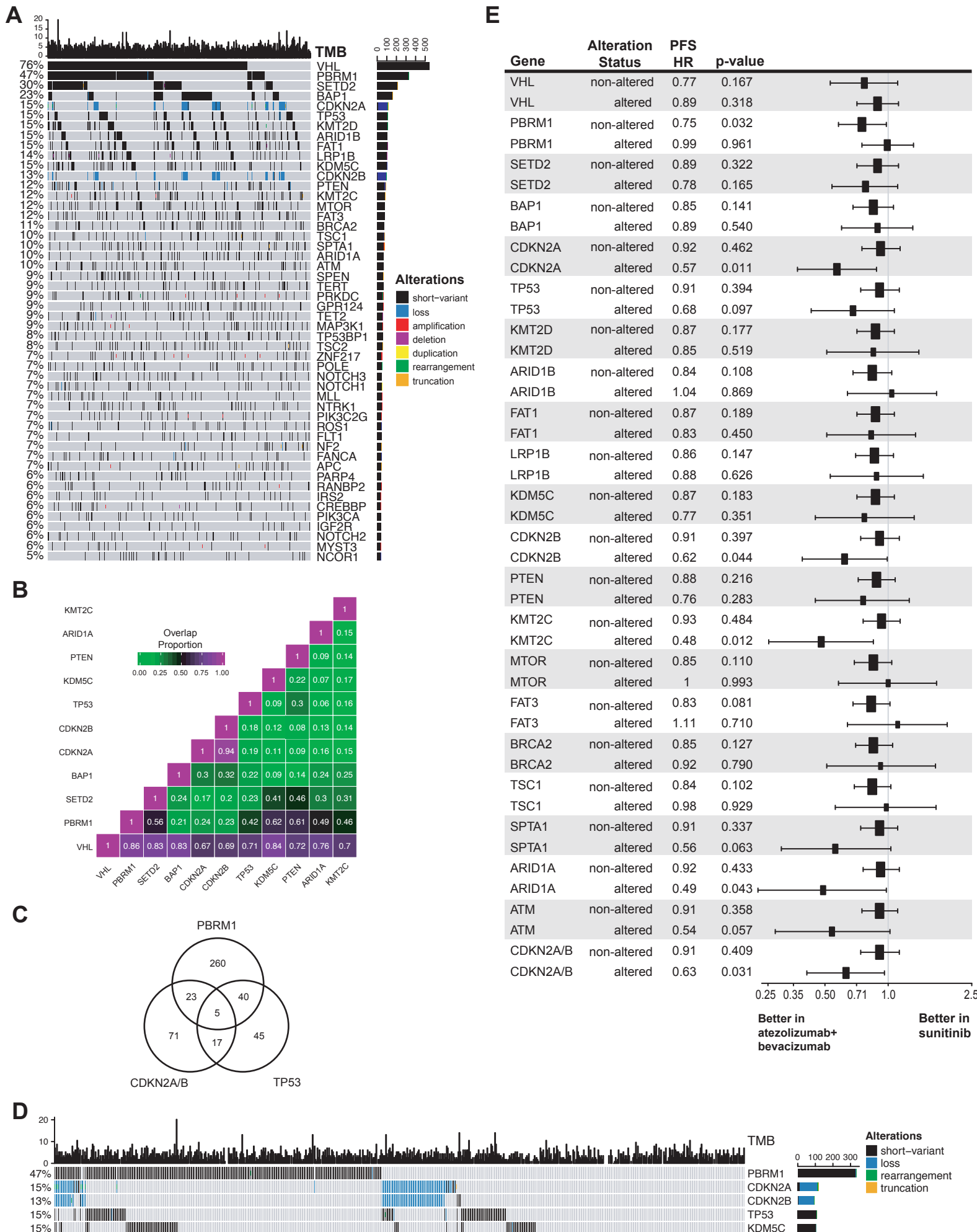
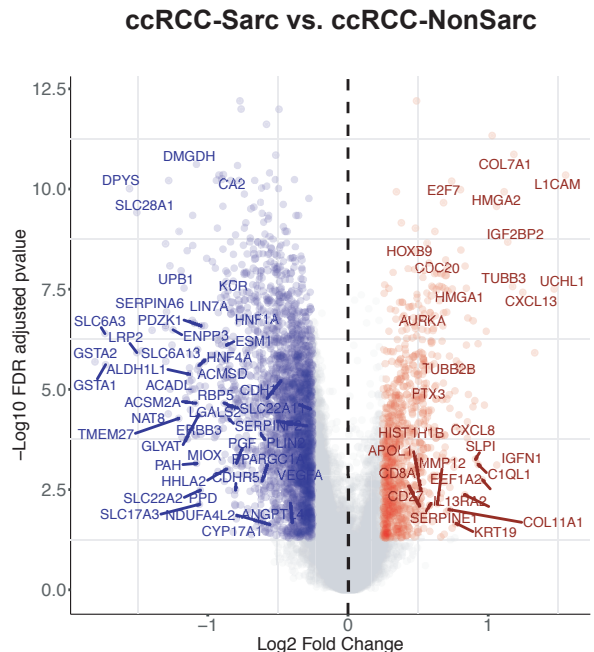


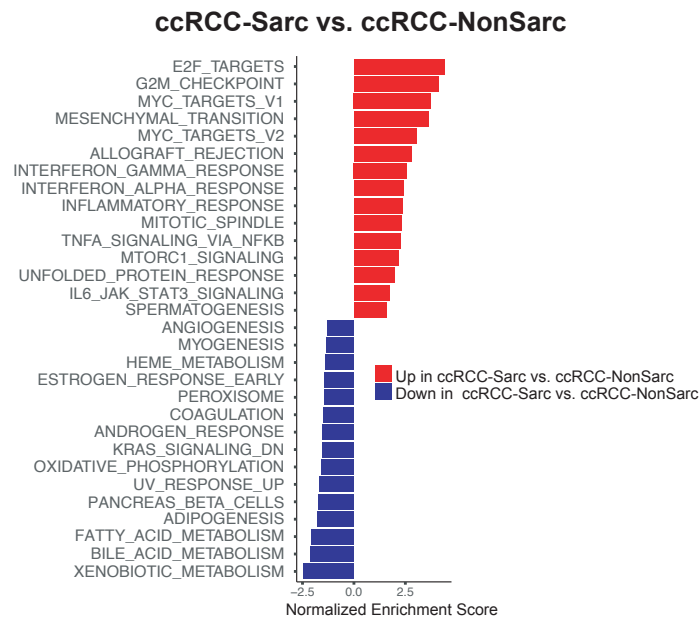
Figure S5: Extended analyses of somatic alterations in tumors from IMmotion 151, Related to Figures 3 and 4. **A.** Oncoprint depicting the top 50 most frequently altered genes in tumors from IMmotion151. **B.** Heatmap representing the overlap proportion between pairs of the most common somatic alterations in this dataset. Proportion is calculated as the ratio of overlap between two groups over the size of the smaller group. The heatmap highlights minimal overlap between PBRM1 mutations and BAP1/CDKN2A/B alterations. **C.** Venn diagram representing the overlap between tumors somatically altered in PBRM1, CDKN2/B and TP53. **D.** Oncoprint depicting somatic alterations in PBRM1, CDKN2A/B, TP53 and KDM5C. **E.** Association between somatic alterations and PFS in genes altered in >10% of tumors. Forest plot depicting PFS hazard ratios comparing patients treated with atezolizumab+bevacizumab vs. sunitinib by somatic alteration status for each gene. Whiskers represent 95% confidence intervals.

Figure S6

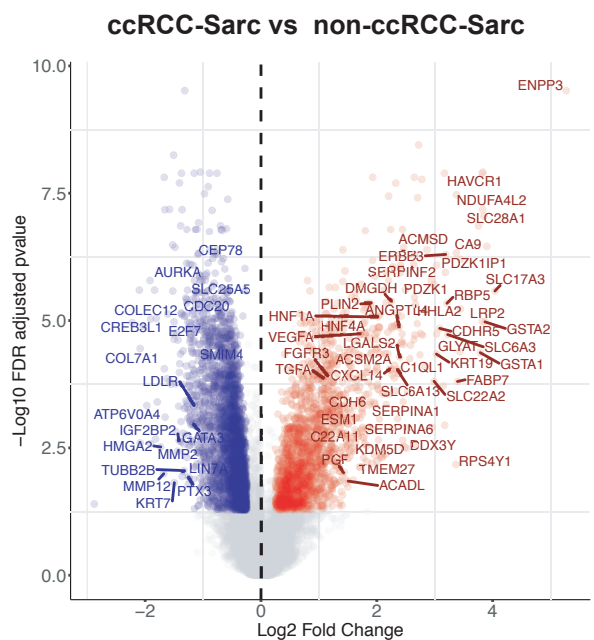
A



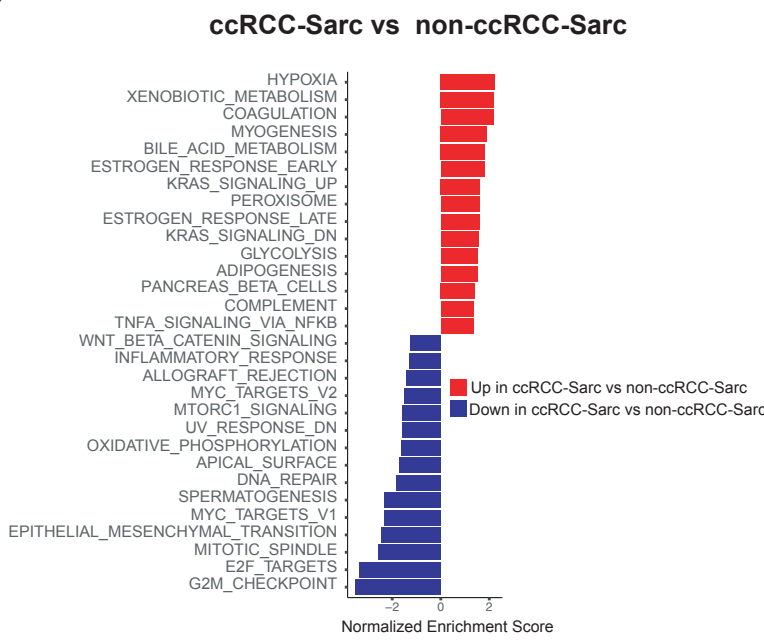
B



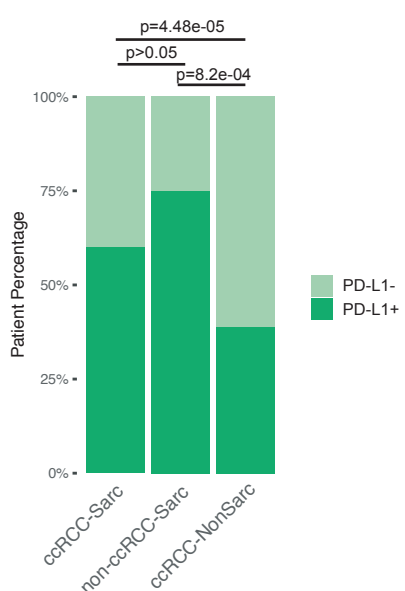
C



D



E



F

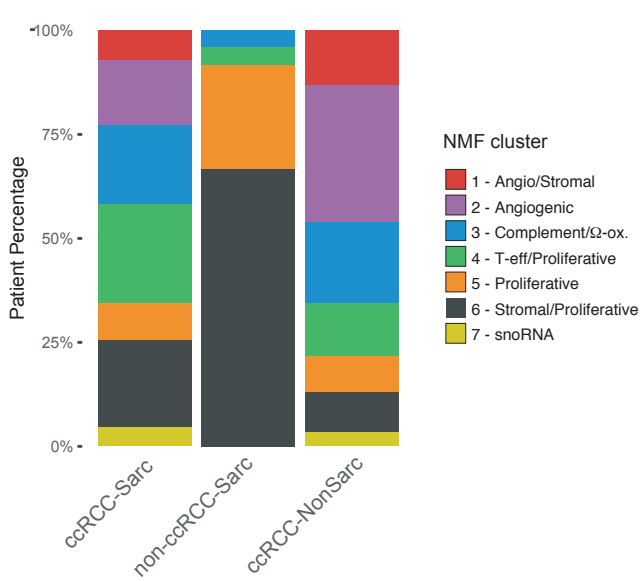


Figure S6: Comparison of molecular features of clear cell RCC sarcomatoid (ccRCC-Sarc), clear cell RCC non-sarcomatoid (ccRCC-NonSarc) and non-clear cell sarcomatoid (non-ccRCC-Sarc tumors, Related to Figure 5. **A.** Volcano plot depicting differentially expressed genes between ccRCC-Sarc and ccRCC-NonSarc tumors. Genes with FDR-corrected $p < 0.05$ and absolute log-fold change ≥ 0.25 are represented in red or blue. **B.** Bar chart representing pathway enrichment scores for the top upregulated or downregulated MSigDb hallmark gene sets within the differentially expressed genes identified in A. **C.** Volcano plot depicting differentially expressed genes between ccRCC-Sarc and non-ccRCC-Sarc tumors. Genes with FDR-corrected $p < 0.05$ and absolute log-fold change ≥ 0.25 are represented in red or blue. **D.** Bar chart representing pathway enrichment scores for the top upregulated or downregulated MSigDb hallmark gene sets within the differentially expressed genes identified in C. **E.** Barchart representing the distribution of PD-L1 expression by immunohistochemistry (IHC) in ccRCC-Sarc, non-ccRCC-Sarc and ccRCC-NonSarc tumors. P-value was obtained from Pearson's Chi-squared test conducted between each pair of conditions. **F.** Barchart representing distribution of non-negative matrix factorization (NMF) clusters in ccRCC-Sarc, non-ccRCC-Sarc and ccRCC-NonSarc tumors.